Contribution from the Department of Chemistry,
The Ohio State University, Columbus, Ohio 43210

A Novel Family of Binuclear Cobalt(II) Complexes with Face-to-Face Bis(cyclidene) Ligands: Structural Characterization, Unusual Reactions with Dioxygen, and a Distinctive Host-Guest Complexation with a Bridging Ligand

Naomi Hoshino, Alan Jircitano, and Daryle H. Busch*

Received August 31, 1987

A series of binuclear cobalt(II) complexes has been prepared and characterized with examples of the family of macrotricyclic ligands containing two metal ion sites that are labeled cyclidene rings. The dimetallic complexes contain a large permanent void bounded by the cyclidene moieties and by two identical bridging groups. The size and shape of the void vary with the bridging groups and are very flexible in solution. The crystal structure of the compound having chloride as the counterion and *m*-xylylene bridging groups reveals the face-to-face structure. The cyclidene groups are offset with respect to each other, and solvent methanol and chloride ion form a pair of hydrogen-bonded bridges across the cavity, between NH groups of the ligand. At low temperatures a dioxygen adduct is formed; however, it autoxidizes more rapidly than the related mononuclear complexes. An unusual form of host-guest complexing has been demonstrated in which 4,4'-bipyridine is both enclosed in the cavity of the bis(cyclidene) complex and coordinated to the two metal atoms, serving as a bridging group and thereby greatly enhancing the metal-metal interaction between the two cobalt(II) atoms.

Introduction

Synthetic multimetal systems are of both fundamental and practical interest. For example, the dicobalt(II) complexes of the *face-to-face* diporphyrin ligands[1,2] have achieved the 4-electron reduction of O_2 to H_2O. Biomimetic models such as this and others[3] reflect the heavy focus of research on multimetallic native systems such as cytochrome *c* oxidase and laccase. Clearly, the presence of four metal centers in the oxidases is not coincidental. On the other hand, Chang and Anson[4] have found that a monocobalt(II) diporphyrin also provides a 4-electron pathway for the electroreduction of O_2. The redox chemistry of dioxygen with dinuclear systems is deserving of much additional research.[5]

We report here a new series of dicobalt(II) *bis(cyclidene)*[6] complexes (structure I), including their syntheses, characterization,

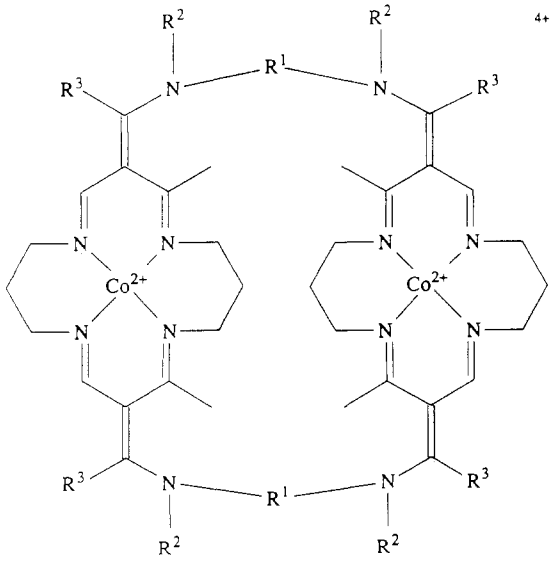

I

and reactions with dioxygen. The X-ray crystal structure of one is both interesting and revealing. The dinickel(II)[7] and diiron(II)[8] analogues have previously been described. Those previous studies on the dinickel(II) bis(cyclidene) complexes produced strong inferences that the R^2 protons of the bridge nitrogens are readily involved in hydrogen-bonding interactions with certain solvents and with halide ions. These interactions are well demonstrated in the results of the X-ray crystal structure determination reported here. The corresponding mononuclear cobalt(II) cyclidene species (so-called lacunar complexes)[9] form remarkably stable and versatile dioxygen adducts with an equimolar ratio of cobalt to O_2. The dinuclear bis(cyclidene) complexes of cobalt(II) react with O_2 in most interesting ways that include both adduct formation and autoxidation.

Table I. ESR Parameters for Dicobalt(II) Bis(cyclidene) Complexes

M	R^1	R^2	solvent/ base	$g_\perp$	$g_\parallel$	$A_\parallel^{Co}$/ G	$A_\parallel^{N}$/ G
Co/CoCl	$(CH_2)_2$	H	acetonitrile		2.21[a]		...
			acetone		2.23[a]		...
			dichloro-methane		2.27[a]		...
			acetonitrile/ 1-MeIm	2.26	1.99	101.0	...
			pyridine	2.29	2.01	100.0	...
Co	$(CH_2)_2$	CH_3	acetonitrile	2.24	2.01	120.0	...
Co	$(CH_2)_3$	H	acetonitrile/ 1-MeIm	2.29	2.01	97.0	...
Co	mxyl	H	acetonitrile	2.26	2.00	117	...
			acetonitrile/ 1-MeIm	2.26	1.98	100.0	...
			pyridine	2.28	2.01	99.8	...
Co	$(CH_3)_2$	*b*	acetonitrile	2.27	2.00	117	13
			pyridine	2.30	2.01	101.7	...
			acetone/ pyridine	2.28	1.99	100.0	14

[a] Broad. Nearly isotropic. [b] Mononuclear unbridged complex, $[Co\{Me_2(NMe_2)_2[16]cyclidene\}]^{2+}$.

Results and Discussion

Synthesis and Characterization. The preparation of the ligand salts and the insertion of the cobalt into the two cyclidene rings follow simple modifications of procedures that are well-known for

(1) Collman, J. P.; Denisevich, P.; Konai, Y.; Marrocco, M.; Koval, C.; Anson, F. C. *J. Am. Chem. Soc.* **1980**, *102*, 6027-6036.
(2) Eaton, S. S.; Eaton, G. R.; Chang, C. K. *J. Am. Chem. Soc.* **1985**, *107*, 3177-3184 and references cited therein.
(3) See for example: Karlin, K. D.; Hayes, J. C.; Gultne, Y.; Cruse, R. W.; McKown, J. W.; Hutchinson, J. P.; Zubieta, J. *J. Am. Chem. Soc.* **1984**, *106*, 2121-2128.
(4) Liu, H. Y.; Abdalmuhdi, I.; Chang, C. K.; Anson, F. C. *J. Phys. Chem.* **1984**, *89*, 665-670.
(5) See: *Selective Recognition and Activation of Small Molecules and Metal Ions in Bioinorganic Chemistry*; Raymond, K. N., Reedijk, J., Eds.; NATO Scientific Affairs Division: Brussels, 1985.
(6) For description of nomenclature see: Goldsby, K. A.; Meade, T. J.; Kojima, M.; Busch, D. H. *Inorg. Chem.* **1985**, *24*, 2588-2590.
(7) Busch, D. H.; Christoph, G. G.; Zimmer, L. L.; Jackels, S. C.; Grzybowski, J. J.; Callahan, R. W.; Kojima, M.; Holter, K. A.; Mocak, J.; Herron, N.; Chavan, M. Y.; Schammel, W. P. *J. Am. Chem. Soc.* **1981**, *103*, 5107-5114.
(8) Herron, N.; Schammel, W. P.; Jackels, S. C.; Grzybowski, J. J.; Zimmer, L. L.; Busch, D. H. *Inorg. Chem.* **1983**, *22*, 1433-1440.
(9) Stevens, J. C.; Jackson, P. J.; Schammel, W. P.; Christoph, G. G.; Busch, D. H. *J. Am. Chem. Soc.* **1980**, *102*, 3283-3285.

0020-1669/88/1327-2292$01.50/0

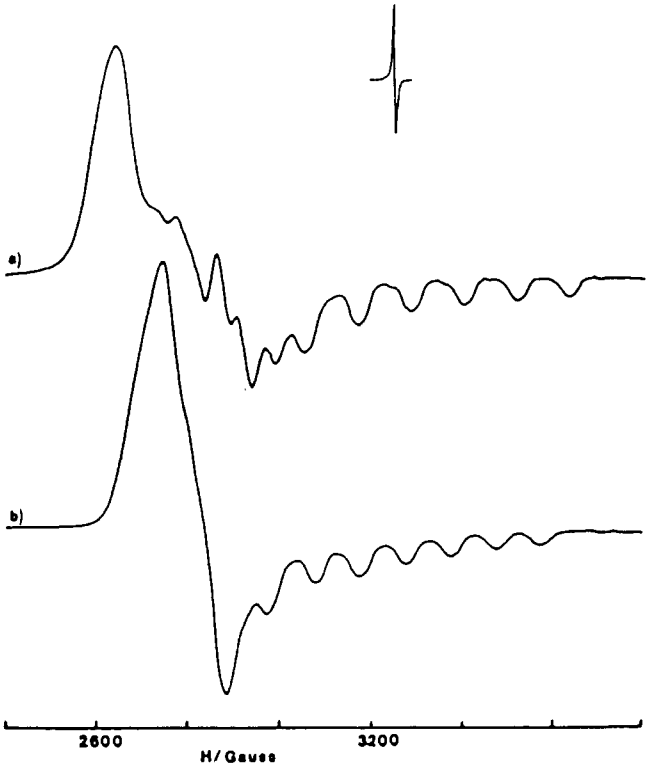

Figure 1. ESR spectra of $[Co_2\{(Me_2(NH)_2mxyl)_2([16]cyclidene)_2\}]^{4+}$: (a) in acetonitrile alone; (b) with excess 1-MeIm added (ESR recorded at 77 K).

the cobalt(II) complexes of other families of cyclidene complexes.[10,11] For the dinucleating bis(cyclidene) ligands, the salts most easily isolated and used are halides, in contrast to the mononuclear cyclidenes that are most often isolated as hexafluorophosphate salts. The most readily isolated form of the metal-free ligand favors the synthesis and characterization of the halide derivatives of the dicobalt complexes.

In the dicobalt(II) complexes reported here, the intermetallic separation is greater than 8 Å; therefore, relatively little metal–metal interaction is expected to be found in studies of the magnetic properties. The magnetic moments were determined in solution by Evans' method and found to lie between 1.90 and 2.09 μ_B/Co and are consistent with the low-spin state of cobalt(II). Figure 1 shows the ESR spectrum of $[Co_2\{(Me_2(NH)_2mxyl)_2([16]cyclidene)_2\}]^{4+}$ (mxyl = *m*-xylylene) as determined in an acetonitrile glass at 77 K, with (b) and without (a) added 1-methylimidazole. These spectra are consistent with a low-spin d^7 structure having axial symmetry and with the unpaired electron occupying the d_{z^2} orbital. $g_\parallel$ is split into eight lines by nuclear hyperfine coupling to the cobalt nucleus and $g_\perp > g_\parallel$. The spectral parameters are reported in Table I. The ESR spectra observed for the closely related mononuclear lacunar cobalt cyclidene complexes are very similar except that superhyperfine splitting, traceable to the presence of a single axial nitrogen donor, is usually observed. Since the dinuclear species fails to show this superhyperfine splitting under identical experimental conditions, its absence may be associated with some metal–metal interaction; e.g., dipolar broadening. Interactions due to the proximities of the two cobalts in the bis(cyclidene) complexes is especially evident in the case of the relatively short $-NHCH_2CH_2NH-$ bridge, where even the cobalt hyperfine structure is poorly defined and the broad spectrum is approximately isotropic in appearance.

X-ray Crystal Structure. The face-to-face bis(cyclidene) complexes have characteristic molecular cavities, between the two metal sites, that are of potential importance in various classes of

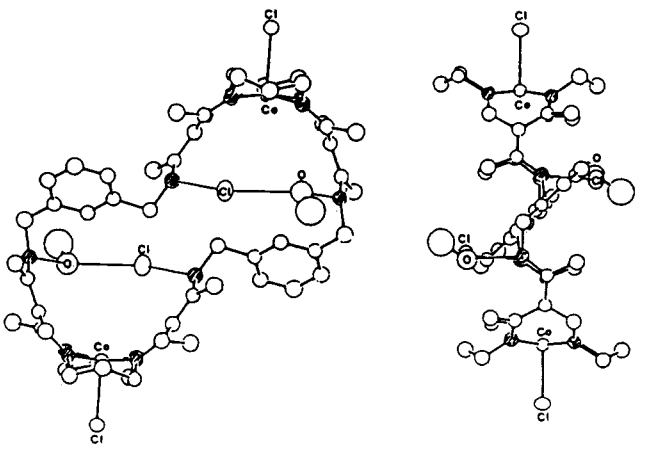

Figure 2. ORTEP diagrams of $[Co_2\{(Me_2(NH)_2mxyl)_2([16]cyclidene)_2\}]Cl_4 \cdot 2CH_3OH$.

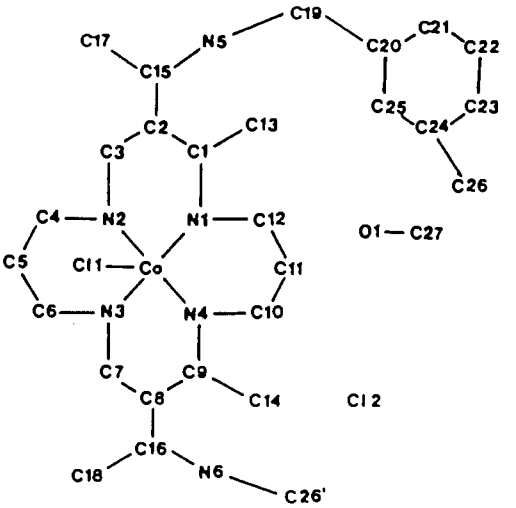

Figure 3. Numbering scheme for dicobalt(II) bis(cyclidene) complex.

inclusion chemistry, the most obvious examples being substrate binding in catalysis and biomimicry and various transport and separation processes. Consequently, it is important to define the dimensions of these cavities. Previously only a single crystal structure has been completed on a bis(cyclidene) complex, $[Ni_2\{(Me_2(NH)_2mxyl)_2([16]cyclidene)_2\}](PF_6)_4 \cdot 2CH_3COCH_3$, and that structure was limited in quality.[12] The dicobalt(II) analogue was subjected to crystal structure determination in this work. This complex salt contained four chlorine atoms, two as chloride counterions and two as axial ligands bound outside the cavity, and methanol molecules.

Two views of the structure of the dicobalt(II) bis(cyclidene) complex are shown in Figure 2. This molecular unit is centrosymmetric, and the two cyclidene centers and the two bridging *m*-xylylene groups are constrained to be equivalent. Considering the most general features first, the side view shows that the cyclidene moieties are indeed face-to-face, with only a slight offset on the basis of that view. Further, the side view shows that the bridging groups proceed in the vertical directions from their points of attachments to the planar bridge nitrogen atoms, a configuration that is described as *lid-on*.[12] The front view (i.e., looking directly into the cavity) shows a substantially greater offset of the two cyclidene moieties. In all of these features, the structure of the dicobalt(II) complex resembles that of the dinickel(II) complex.[7] Because of the presence of the coordinated chloride as an external fifth ligand on each cobalt atom (Co–Cl = 2.55 Å), the two saturated chelate rings (Co–N1–C12–C11–C10–N4 and Co–N2–C4–C5–C6–N3; for numbering scheme, see Figure 3) both

(10) Busch, D. H.; Olszanski, D. J.; Stevens, J. C.; Schammel, W. P.; Kojima, M.; Herron, N.; Zimmer, L. L.; Holter, D. K. A.; Mocak, J. *J. Am. Chem. Soc.* **1981**, *103*, 1472–1478.
(11) Takeuchi, K. J. Ph. D. Thesis, The Ohio State University, 1979.
(12) Hoshino, N.; Goldsby, K. A.; Busch, D. H. *Inorg. Chem.* **1986**, *25*, 3000–3006.

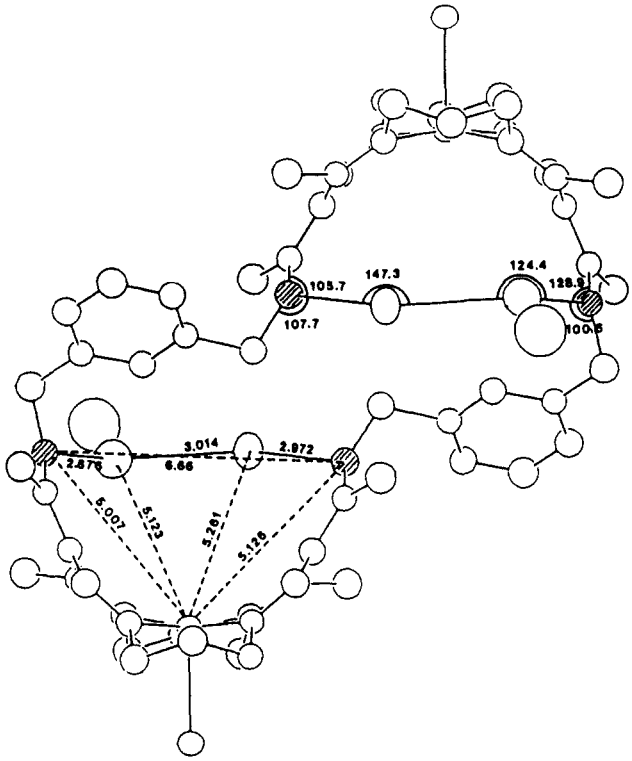

Figure 4. Dimensions of the hydrogen-bonding arch in $[Co_2\{(Me_2(NH)_2mxyl)_2([16]cyclidene)_2\}]Cl_4 \cdot 2CH_3OH$.

adopt chair conformations. With only a void in the external coordination location, one of the corresponding rings in the dinickel(II) complex assumes a boat conformation. Similarly, other cyclidene structures in which the external coordination site is occupied display pairs of chair conformations (chloro–iron(II)[13] and thiocyanato–cobalt(III)[14]).

Although the vertical interplanar separation between the two cyclidene rings (N_4 plane) is only 10.70 Å, the large horizontal, or shear, displacement (6.24 Å) of the two cyclidene units causes the two cobalt atoms to be separated by 12.38 Å. It follows that the cross sectional shape of the cavity is approximated better by a parallelogram than by a tall rectangle. This horizontal distortion is less severe in the dinickel structure (Ni–Ni = 13.6 Å; plane–plane = 12.8 Å; shear displacement = 4.6 Å).

The most remarkable feature revealed by the ORTEP drawings is the precise hydrogen bonding within each bis(cyclidene) unit. Each pair of NH groups in the –NH–mxyl–NH– bridging unit is spanned by a hydrogen-bonded chain including one chloride ion and one molecule of methanol. These chains arch out from the cavity and more or less block one side of the cavity. Figure 4 displays the dimensions of this hydrogen-bonding arch.

The N5–O, O–C12, and C12–N6 lengths are all consistent with literature values of 2.57–3.22 Å for nitrogen–H–oxygen, 2.86–3.21 Å for oxygen–H–halide, and 2.91–3.52 Å for halide–H–nitrogen bondings.[15] An apparent consequence of this hydrogen-bonding chain is that the N5–N6 distance is significantly elongated (6.66 Å) as compared to that in the dinickel(II) species (5.74 Å). No such hydrogen-bonding interaction was found in the structure of the dinickel(II) compound. The presence of the chloride ions may be credited with two major distortions in the structure of the dicobalt(II) structure: the occurrence of pairs of chain conformers for the saturated rings of the cyclidene moieties and the expanded shear displacement associated with the hydrogen-bonding chains. These changes reflect the substantial flexibility of the bis(cyclidene) structure, a subject that has also been addressed in connection with solution studies.[6]

The structural relationships shown in the front view in Figure 2 bear a fascinating resemblance to the structure of *m*-xylylene-bridged mononuclear lacunar complexes. If one focuses attention on a single cyclidene moiety, it is soon realized that one of the *m*-xylylene bridging groups is oriented in a position very similar to the roof of the lacuna in the related mononuclear lacunar complex. Thus, even the configuration of the complexes of the dimeric ligand gives evidence for the propensity to form the lacunar complexes. The shape relationships that favor ring closure in the monomeric complexes generate the shear distortion of the dinuclear congenors. Additional bond length and bond angle data are listed in Tables II and III. Final positional parameters are given in Table IV.

While details of the solid-state structures may not be completely transferable to solution behavior, an important inference derived from the precise hydrogen-bonded chains in the structure of this dicobalt(II) complex relates very generally to the character of the large permanent void in the structure. Hydrogen bonding to the hydrogen atoms of the NH groups in the bridge (R^2 in structure I) could make the cavity much less hydrophobic than would otherwise be the case. Replacement of this hydrogen with alkyl groups (N-alkylation of the bridge groups) is expected to enhance the hydrophobic nature of the cavity and, for example, deter interaction of hydrogen-bonding solvents with coordinated dioxygen.

Table II. Bond Length and Other Distance Data (Å) for $[Co_2\{(Me_2(NH)_2mxyl)_2([16]cyclidene)_2\}]Cl_4 \cdot 2CH_3OH$

Co–Cl1	2.546 (4)	C10–C11	1.526 (23)
Co–N1	1.947 (12)	C11–C12	1.496 (24)
Co–N2	1.926 (13)	C15–C17	1.514 (22)
Co–N3	1.948 (11)	C15–N5	1.343 (18)
Co–N4	1.968 (12)	C16–C18	1.511 (22)
N1–C1	1.307 (19)	C16–N6	1.343 (18)
N1–C12	1.485 (21)	C19–N5	1.480 (19)
N2–C3	1.297 (18)	C19–C20	1.527 (22)
N2–C4	1.482 (19)	C20–C21	1.381 (22)
N3–C6	1.471 (18)	C20–C25	1.419 (22)
N3–C7	1.281 (19)	C21–C22	1.408 (23)
N4–C9	1.294 (19)	C22–C23	1.390 (24)
N4–C10	1.469 (21)	C23–C24	1.396 (21)
C1–C2	1.459 (21)	C24–C25	1.355 (20)
C1–C13	1.552 (22)	C24–C26	1.576 (22)
C2–C3	1.443 (21)	C26′–N6	1.483 (19)
C2–C15	1.392 (19)	C27–O1	1.384 (31)
C4–C5	1.561 (23)	Co···Co	12.384 (2)
C5–C6	1.549 (24)	vert	10.696
C7–C8	1.498 (22)	horiz	6.242
C8–C9	1.442 (21)	C26···C26′	3.35
C8–C16	1.374 (20)		
C9–C14	1.526 (23)		

Table III. Bond Angles (deg) for $[Co_2\{(Me_2(NH)_2mxyl)_2([16]cyclidene)_2\}]Cl_4 \cdot 2CH_3OH$

N2–Co–N1	88.0 (5)	C16–C8–C9	124.6 (14)
N4–Co–N1	91.4 (5)	C8–C9–N4	123.1 (14)
N3–Co–N2	89.8 (5)	C14–C9–N4	120.1 (13)
N4–Co–N3	88.9 (5)	C14–C9–C8	116.0 (13)
C1–N1–Co	123.3 (10)	C11–C10–N4	110.6 (13)
C12–N1–Co	117.6 (9)	C12–C11–C10	113.4 (13)
C3–N2–Co	123.6 (9)	C11–C12–N1	110.2 (12)
C4–N2–Co	121.4 (9)	C17–C15–N5	115.6 (12)
C6–N3–Co	122.6 (9)	C17–C15–C2	123.4 (12)
C7–N3–Co	122.0 (9)	N5–C15–C2	120.8 (13)
C9–N4–Co	123.8 (11)	C18–C16–N6	117.5 (12)
C10–N4–Co	115.0 (10)	C18–C16–C8	125.0 (12)
C2–C1–N1	119.7 (13)	N6–C16–C8	117.6 (13)
C13–C1–N1	122.7 (13)	C19–N5–C15	126.4 (12)
C13–C1–C2	116.7 (13)	C26′–N6–C16	125.6 (12)
C3–C2–C1	120.0 (12)	C20–C19–N5	109.3 (12)
C15–C2–C1	121.6 (12)	C21–C20–C19	120.1 (14)
C15–C2–C3	118.4 (13)	C21–C20–C25	119.1 (14)
C2–C3–N2	119.8 (14)	C25–C20–C19	120.8 (13)
C5–C4–N2	109.7 (12)	C22–C21–C20	120.9 (15)
C6–C5–C4	111.9 (13)	C23–C22–C21	119.3 (15)
C5–C6–N3	110.1 (11)	C24–C23C22	118.8 (14)
C8–C7–N3	123.8 (13)	C25–C24–C23	122.4 (14)
C9–C8–C7	116.7 (12)	C26–C24–C25	117.6 (13)
C16–C8–C7	118.5 (13)	C24–C25–C20	119.3 (14)

(13) Zimmer, L. L. Ph. D. Thesis, The Ohio State University, 1979.
(14) Jackson, P. J. Ph. D. Thesis, The Ohio State University, 1981.
(15) Stout, G. H.; Jensen, L. H. *X-Ray Structure Determination: a Practical Guide*; MacMillan: New York, 1968; p 303.

Table IV. Atomic Coordinates for $[Co_2\{(Me_2(NH)_2mxyl)_2([16]cyclidene)_2\}]Cl_4 \cdot 2CH_3OH$

atom	x	y	z
Co	0.3015 (2)	0.2406 (2)	0.2274 (1)
Cl1	0.5036 (3)	0.3066 (3)	0.2876 (2)
Cl2	0.0571 (4)	0.2520 (4)	−0.0181 (2)
N1	0.2168 (11)	0.3647 (9)	0.2136 (6)
N2	0.2343 (10)	0.2263 (8)	0.3091 (5)
N3	0.3550 (10)	0.1054 (8)	0.2343 (6)
N4	0.3449 (9)	0.2452 (10)	0.1366 (5)
N5	−0.1431 (10)	0.3212 (8)	0.1936 (6)
N6	0.1733 (10)	0.0460 (9)	0.0110 (6)
C1	0.1076 (13)	0.3794 (11)	0.2279 (7)
C2	0.0496 (12)	0.3042 (10)	0.2630 (7)
C3	0.1219 (12)	0.2459 (13)	0.3139 (7)
C4	0.3031 (14)	0.1774 (12)	0.3687 (8)
C5	0.3286 (14)	0.0694 (12)	0.3513 (8)
C6	0.4138 (12)	0.0619 (10)	0.2978 (7)
C7	0.3313 (13)	0.0458 (11)	0.1851 (8)
C8	0.2945 (14)	0.0769 (11)	0.1136 (8)
C9	0.3343 (13)	0.1719 (11)	0.0958 (7)
C10	0.3996 (15)	0.3371 (12)	0.1192 (8)
C11	0.3088 (15)	0.4206 (12)	0.1181 (8)
C12	0.2812 (14)	0.4464 (12)	0.1861 (8)
C13	0.0441 (14)	0.4803 (12)	0.2205 (8)
C14	0.3848 (14)	0.1782 (12)	0.0300 (8)
C15	−0.0758 (13)	0.2895 (10)	0.2507 (7)
C16	0.2347 (12)	0.0110 (10)	0.0688 (7)
C17	−0.1440 (13)	0.2327 (12)	0.2971 (7)
C18	0.2365 (14)	−0.0980 (12)	0.0784 (8)
C19	−0.2715 (14)	0.2955 (12)	0.1685 (8)
C20	−0.2788 (13)	0.1886 (11)	0.1476 (7)
C21	−0.3651 (14)	0.1284 (11)	0.1683 (8)
C22	−0.3707 (14)	0.0289 (12)	0.1513 (8)
C23	−0.2888 (13)	−0.0087 (11)	0.1126 (7)
C24	−0.2058 (12)	0.0542 (10)	0.0898 (7)
C25	−0.1985 (13)	0.1499 (11)	0.1063 (7)
C26	−0.1118 (13)	0.0135 (11)	0.0458 (7)
C27	0.8584 (26)	0.0616 (22)	0.5255 (15)
O1	0.9355 (11)	0.1172 (10)	0.5712 (6)

Reaction with O_2. First of all, it should be recalled that the present dicobalt(II) species have flexible cavities that are large enough to preclude strong metal–metal interactions. This also eliminates the possibility that the two cobalt(II) ions might simultaneously bind to the same O_2 molecule. Consequently, this large separation between the pairs of metal atoms leads to the expectation that each of the cobalt centers should combine with O_2 in a 1:1 mole ratio.

Usually the electrochemical potential of the Co^{3+}/Co^{2+} couple serves as a credible indicator of the probable O_2 affinity of a cobalt(II) oxygen carrier.[16] Unfortunately, these particular cobalt bis(cyclidene) complexes display irreversible Co^{3+}/Co^{2+} couples; however, the values observed for their oxidation peak potentials (0.27–0.37 V vs $Ag/AgNO_3$ in acetonitrile) are similar to those of the mononuclear lacunar cyclidene complexes.[17] This suggests that the two families of cobalt cyclidene complexes might have similar intrinsic affinities for O_2. Earlier studies have shown that large cavities produce the maximum O_2 affinities, and since large cavities separate the pairs of cobalt ions in these dinuclear cyclidene complexes, large O_2 affinities are expected; i.e., $P_{50} \leq 2$ Torr at room temperature.[18]

Because all known oxygen carriers undergo autoxidation (oxidation by O_2), the expected behavior of these dinuclear complexes with O_2 is complicated. For clarity, the experimental studies to follow make use of the reaction sequence given in Scheme I. This scheme illustrates the pertinent chemical reactions available to the subject systems. Most generally, they are oxygen adduct forming processes and autoxidation processes. O_2 adduct formation can be studied when the rates of the autoxidation processes

Scheme I

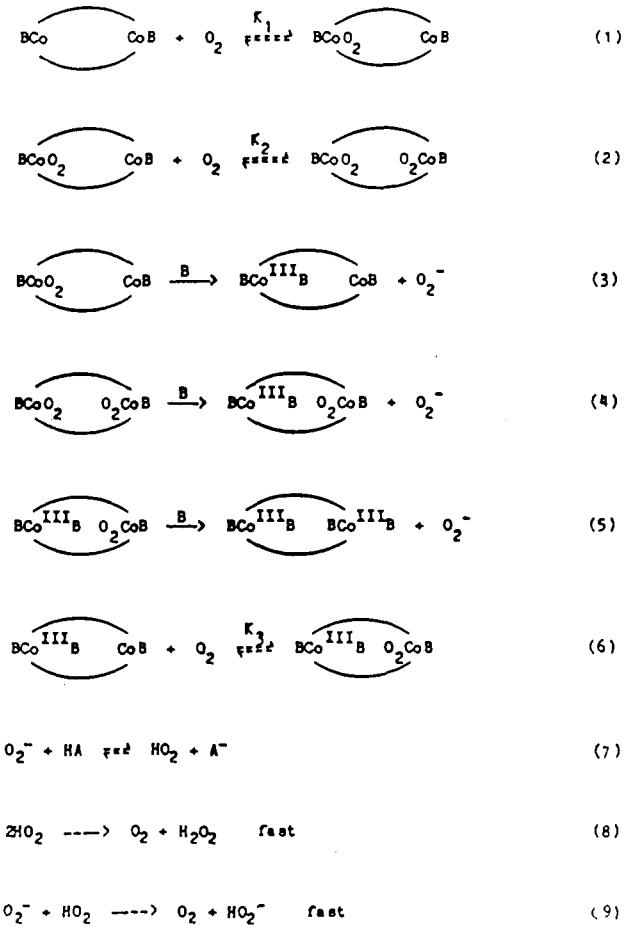

are slow on the time scale that permits observation of the oxygen adduct.

Reactions 1 and 2 in Scheme I represent the successive reversible binding of two dioxygen molecules. Appropriate axial bases, B, are presumed to be coordinated to the cobalt atoms. Either or both of these dioxygen adducts (from eq 1 or 2) will undergo irreversible autoxidation at some, as yet undetermined, rate. Equations 3–5 represent such autoxidation processes and, for simplicity, it is assumed that the products of autoxidation are a 6-coordinate cobalt(III) center and superoxide ion. We are mainly concerned here with elucidating the oxygen binding processes. Reactions 3 and 4 produce unusual mixed valence species, in (3) the cobalt(II) is in the deoxy form while in (4) it is in the oxygenated form. This cobalt(II) center may be viewed as a unique lacunar complex, whose cavity size is determined in large part by the presence therein of the third mole of axial ligand B (which is coordinated to the other cobalt center). Equation 6 describes the oxygenation reaction for that new lacunar species (the product of both reactions 3 and 4). Finally, it should again be emphasized that two widely separated cobalt sites are expected to be independent of each other with the result that neither the stepwise binding of O_2 nor the mixed valence (Co^{II}/Co^{III}) intermediate need necessarily be experimentally obvious. Since we are able to vary the separation between the two cobalt centers, we might hope to gain information about how great a separation is required to produce the expected independence.

The reactions between the cobalt bis(cyclidene) complexes and O_2 have been studied in acetonitrile solvent in the presence of 1-methylimidazole. Figure 5 shows the changes in the ESR spectrum as oxygen reacts with the *m*-xylylene-bridged complex at room temperature. The axial spectrum attributable to the pentacoordinate low-spin cobalt(II) complex simply diminishes with time upon exposure of the solution to air and disappears completely after 60 s. Also, there is no trace of the distinctive ESR spectrum expected for a 1:1 cobalt/O_2 adduct at any time during the process. This rapid autoxidation and failure to observe

(16) Carter, M. J.; Rillema, D. P.; Basolo, F. *J. Am. Chem. Soc.* **1974**, *96*, 392–400.
(17) Chavan, M. Y.; Meade, T. J.; Busch, D. H.; Kuwana, T. *Inorg. Chem.* **1986**, *25*, 314–321.
(18) Busch, D. H. In *Oxygen Complexes and Oxygen Activation by Transition Metals*; Martell, A. E., Ed.; Plenum: New York, 1988; pp 61–85.

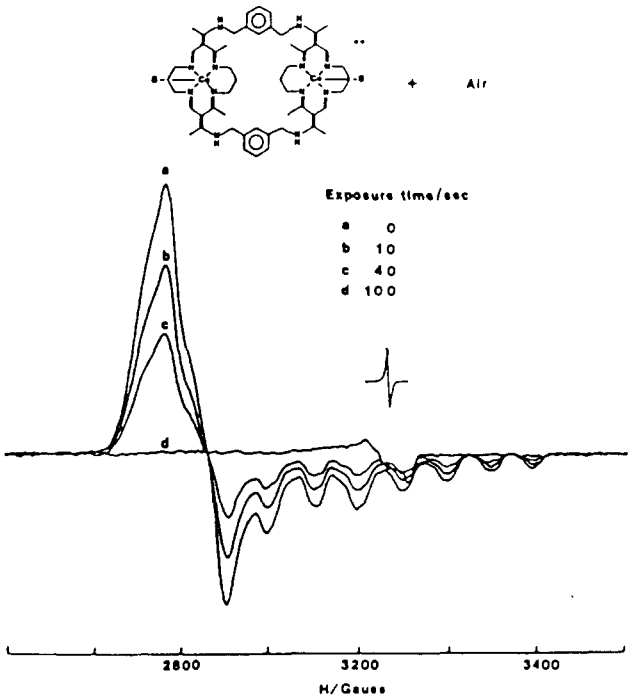

Figure 5. Changes in ESR that accompany the reaction of $[(Co(1\text{-MeIm}))_2\{(Me_2(NH)_2mxyl)_2([16]cyclidene)_2\}]^{4+}$ with air at room temperature (in acetone containing 1-MeIm; ESR recorded at 77 K).

an O_2 adduct is in marked contrast to behavior of the lacunar family of cobalt(II) oxygen carriers. For example, lacunar $[Co(1\text{-MeIm})\{Me_2(NR^2)_2(CH_2)_6[16]cyclidene\}]^{2+}$ complexes form O_2 adducts that autoxidize with half-lives of 4100 (R^2 = H) and 6300 s ($R^2 = CH_3$), respectively, at 20 °C. It seems irrational to suppose that the dicobalt(II) complexes fail to bind O_2, but the irreversible autoxidation of the complexes is obviously so very rapid that it completely dominates their room-temperature behavior. Referring to Scheme I, it follows that the O_2 adduct forming reactions (eq 1 and 2) are accompanied by very rapid autoxidation reactions of the types indicated by eq 3–5.

In contrast, the formation of the dioxygen adduct by the *m*-xylylene-bridged dicobalt(II) species was easily observed at low temperatures. Figure 6 shows the use of ESR to track the time course of formation and decomposition of the dioxygen adduct of the *m*-xylylene derivative $[\{Co(1\text{-MeIm})\}_2\{(Me_2(NH)_2mxyl)_2([16]cyclidene)_2\}]^{4+}$ at −40 °C in the presence of 0.1 Torr of dioxygen. Spectrum a shows the typical spectrum of an oxygen-free, tetragonal low-spin cobalt(II) species. Upon the addition of the low partial pressure of oxygen (0.1 Torr), this signal almost completely disappears and is replaced by a spectrum that definitively shows the presence of the 1:1 O_2 adduct (spectrum b). The axial signal at $g \cong 2$ ($g_\perp$ = 1.98, $g_\parallel$ = 2.05, and $A_\parallel^{Co}$ = 16.7 G) is characteristic of the 1:1 Co/O_2 adducts.[9] This complete replacement of the deoxy spectrum by the O_2 adduct spectrum by a system in equilibrium with 0.1 Torr of oxygen provides evidence that the O_2 affinity of the complex is great, as expected.

Signal intensity relationships also provide information about the reactions that have occurred in this system. The observed intensity of the O_2 adduct signal does not account for all of the cobalt that is present. As a rule of thumb, the maximum amplitudes of the ESR signals for the 1:1 Co/O_2 adducts are about 10 times those for the corresponding deoxy, low-spin cobalt(II) complexes. On this basis, the observed signal (after 20-s exposure time) accounts for roughly 20%, at most, of the cobalt that is known to be present. This signal disappears with time, and exposure to pure oxygen does not fully restore its intensity. Two possible reactions would account for the loss of ESR signal intensity: (1) irreversible autoxidation or (2) reversible formation of a dimeric peroxo-bridged species. The addition of an atmosphere of oxygen is expected to reverse the latter process but not

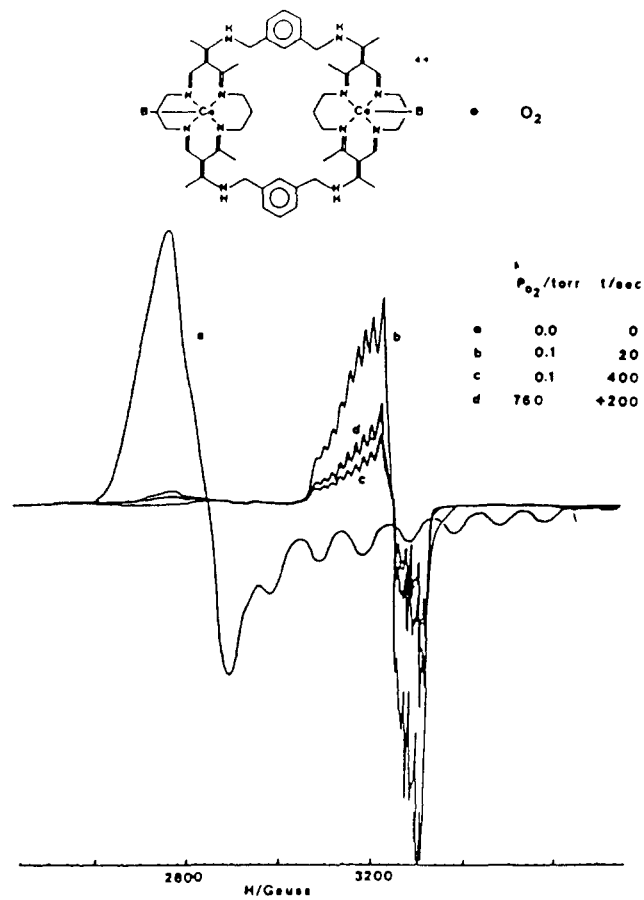

Figure 6. ESR spectral changes that accompany the reaction of $[(Co(1\text{-MeIm}))_2\{(Me_2(NH)_2mxyl)_2([16]cyclidene)_2\}]^{4+}$ with O_2/N_2 at −40 °C (in acetone containing 1-MeIm; ESR recorded at 77 K).

the former. Consequently, it is concluded that extensive autoxidation has occurred during a very short time.

The complex having the shorter $Me_2(NH)_2CH_2CH_2$ bridge exhibited a different behavior at low temperature. The reaction of this complex with 0.1 Torr of oxygen at −45.2 °C was monitored by ESR spectroscopy and the results are summarized in Figure 7. In contrast to the previously described case, much of cobalt(II) forms the 1:1 O_2 adduct. Further, this adduct appears to persist at this low temperature.

Figure 7a shows the spectrum of the starting low-spin deoxy cobalt(II) complex, and figure 7b shows that after brief exposure (20 s) to 0.1 Torr of O_2 only the deoxy spectrum is observed but it is changed in most significant ways: (1) its intensity is significantly diminished, and (2) resolution is substantially improved so that we now observe the superfine splitting due to coupling of the unpaired electron with the nuclear spin of the axial ligand.

Failure to observe the expected nitrogen superhyperfine coupling (attributable to the imiadazole ligand) in the initial spectrum of the cobalt(II) complex is traceable to the close proximity of the two paramagnetic cobalt(II) centers. The subsequent resolution of this superhyperfine splitting after exposure of the solution to 0.1 Torr of oxygen for 20 s may be rationalized in terms of eq 3 or 4 of Scheme I. Thus, the autoxidation proceeds rapidly for one of the two cobalt(II) centers in this dinuclear species, and this produces a compound having a single paramagnetic center, which necessarily produces a more highly resolved ESR spectrum. Furthermore, this selective process is readily understood on the basis of the detailed structure of the compound. Structure II

II

represents such a mixed-valence compound. The short dimethylene

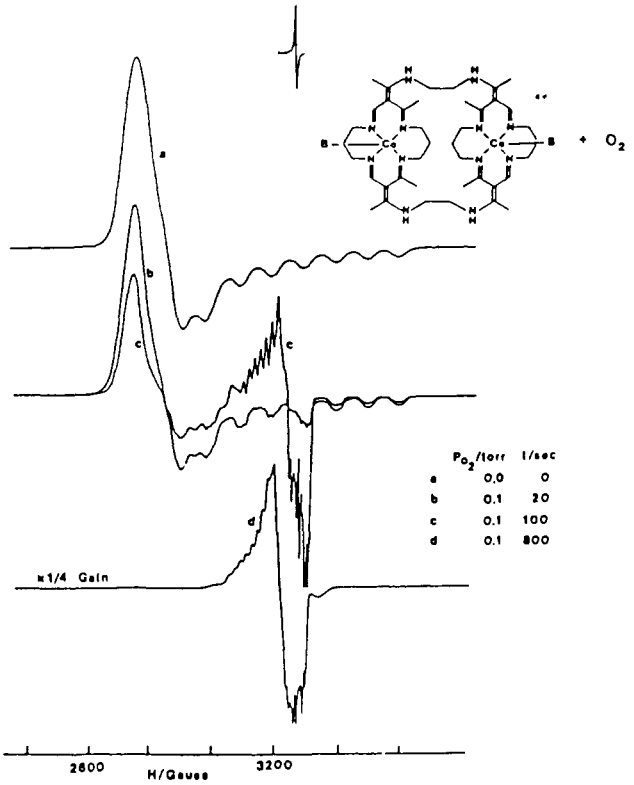

Figure 7. ESR spectral changes that accompany the reaction of $[(Co(1\text{-MeIm}))_2\{(Me_2(NH)_2CH_2CH_2)_2([16]cyclidene)_2\}]^{4+}$ with O_2/N_2 at −45.3 °C (in acetone containing 1-MeIm; ESR recorded at 77 K).

bridge produces a relatively small cavity between the two cobalt centers and this is adequate to accommodate only one of the relatively large 1-methylimidazole ligands required to produce a stable cobalt(III) center. Consequently only one center is oxidized. It is equally interesting that the presence of a single oxidized center greatly reduces the size of the cavity in the vicinity of the remaining cobalt(II) ion. This smaller lacuna is better suited to the formation of stable O_2 adducts as has previously been shown in many systems.[18]

Subsequent exposure of the system to 0.1 Torr of O_2 for longer periods of time (spectrum c, 100 s) is accompanied by the appearance of the spectrum of the O_2 adduct, along with that of the deoxy compound. Eventually (spectrum d, 800 s), all of the low-spin cobalt(II) signal disappears, and only the oxygen adduct is evidenced by the ESR pattern. Further, the maximum amplitude of the signal intensity associated with the O_2 adduct, at this point, is about 3.7 times that of the initial cobalt(II) spectrum. On the basis of the semiquantitative relationship stated earlier, this shows that a substantial fraction of the cobalt is still present as the oxygen adduct. Thus, the oxygen adduct is a major constituent of the system and it is relatively long-lived. These points are all consistent with the proposed formation of a mixed-valence compound that is a relatively good oxygen carrier.

The bis(dimethylene)-bridged species has also been studied in the absence of strong axial bases, such as 1-MeIm. Exposure of an acetone or dichloromethane solution of the $Me_2(NH)_2CH_2CH_2$ derivative to an atmosphere of oxygen at −46 °C produces a broad, intense, poorly resolved ESR spectrum centered at $g = 2$. The wide peak-to-peak separation (80–130 G) argues against an organic radical as its source, and the great amplitude is some 10–12 times that of the initial cobalt(II) signal. It is suggested that the great signal strength implies O_2 adduct formation at both cobalt centers and that the extensive broadening in the spectrum may be due to interactions between the two Co/O_2 moieties in close proximity.

The reversibility of the dioxygen binding in this system has been demonstrated, and this strongly supports the interpretation presented above for the ESR observations. Figure 8 shows the changes in absorption spectrum that accompany successive

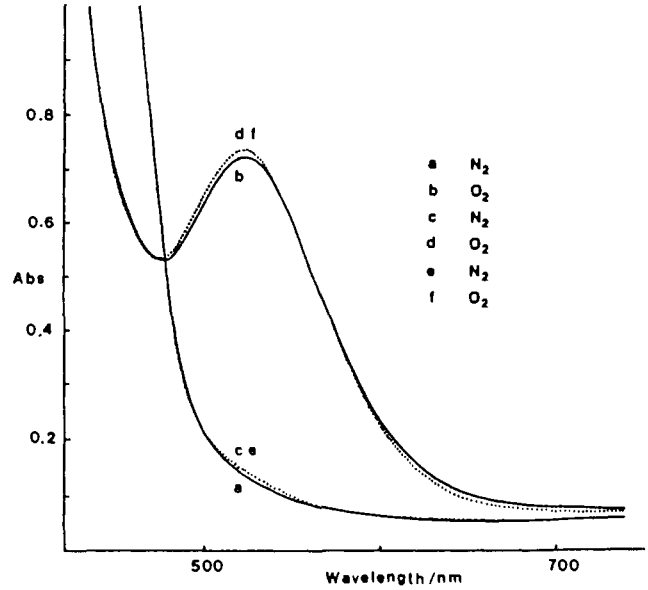

Figure 8. Visible absorption spectral changes showing reversible oxygenation of $[Co_2\{(Me_2(NH)_2CH_2CH_2)_2([16]cyclidene)_2\}]^{4+}$ in acetone at −44.1 °C.

equilibration with atmospheres of nitrogen and then of oxygen for the dimethylene-linked dicobalt(II) complex, in acetone solution. The visible spectrum of the unoxygenated solution is featureless. When pure oxygen is bubbled through the solution at −44.1 °C for 120 s, a strong band grows in at 522 nm. This band disappears completely when the solution is purged with nitrogen. Clearly, the process is reversible at this low temperature. Similar experiments using various partial pressures of oxygen have led to an estimate of $P_{50} = 10$ Torr for this complex. In summary, the behavior of this system at −46 °C is totally described by eq 1 and 2 of Scheme I. Only oxygen adduct formation is observed with no evidence of autoxidation under these conditions.

It is important at this point to summarize the conclusions of the several studies described above. The bis(cyclidene) dicobalt(II) complexes are rapidly autoxidized at room temperature, and no evidence is found for O_2 adducts. Studies at lower temperatures with the *m*-xylylene-bridged dicobalt system, clearly show that some 1:1 O_2 adduct does indeed form (Scheme I, eq 1 and 2) and that the adduct is associated with the expected large oxygen affinity (since it saturates so readily at so low a partial pressure of O_2). Further, the complex autoxidizes (eq 3–5) to a diamagnetic species very rapidly, even at −40 °C (since so much of the cobalt has become ESR silent so quickly). The dicobalt(II) complex having relatively short dimethylene bridges behaves quite differently. In the absence of the *N*-methylimidazole axial ligand, the binding of O_2 is completely reversible at low temperatures and the oxygen affinity is modest, as would be expected. Only eq 1 and 2 of Scheme I are required to describe this behavior. In contrast, in the presence of the axial base, irreversible oxidation of one of the cobalt(II) centers is extremely rapid and there is some evidence that the second center persists in the form of its oxygen adduct. Thus, we describe this system in terms of eq 1, 2, 4, and 6. The variation in cobalt–cobalt distance is responsible for a number of observed differences in spectroscopic and chemical properties.

Axial Base Inclusion Complex. The concept of host–guest association was originally developed for a large domain of purely organic systems, but the host–guest association can include coordination of the guest molecule to one or more metal atoms in the host molecule.[19] Such an inclusion complex has been prepared and isolated in this study. The bridging ligand 4,4′-bipyridine has been included within the cavity of the *m*-xylylene-bridged dicobalt bis(cyclidene) complex (structure III). The ESR spectrum of the dicobalt(II) complex (acetone glass at 77 K)

(19) Meade, T. J.; Busch, D. H. *Prog. Inorg. Chem.* **1985**, *33*, 59–125.

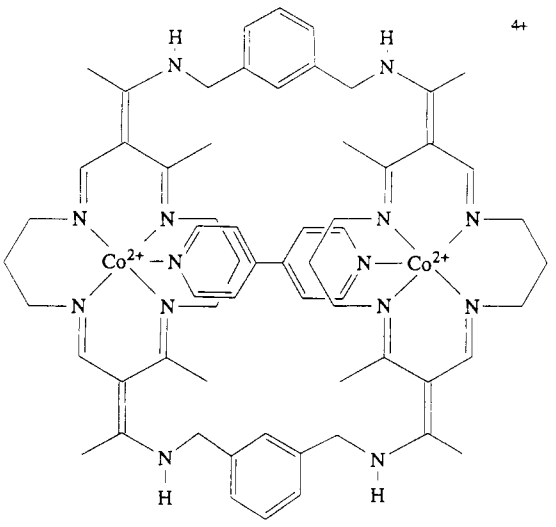

III

provides clear evidence for the coupling between the two cobalt(II) centers (Figure 9). The cobalt hyperfine coupling in the parallel branch of the spectrum is consistent with the interaction of an electron with two cobalt nuclei ($g_{\parallel} = 2.03$, $g_{\perp} = 2.29$, $A_{\parallel}^{Co} = 52.6$ G). Zero-field splitting is not observed in either the $g_{\parallel}$ or the $g_{\perp}$ region. This is reasonable in view of the intermetallic distance required by the included bridging ligand (11.7 Å, estimated from Ru–bpy–Ru[20]). The 4,4′-bipyridine mediation of the exchange coupling may be via a σ-pathway. The d_{z^2} orbitals of the cobalt atoms should have net overlap with the σ bonds of the bridging ligand, not the π system. Magnetic moment determinations by the Evans method in acetonitrile solution gave results (2.08–2.18 μ_B/Co) slightly but definitely higher than those for the host alone. Interestingly, these data correspond to 2-electron magnetic moments of slightly greater than 3 μ_B, numbers commonly associated with two coupled spins on single first-row transition-element atoms. Controlled-potential electrolysis at ~0.5 V vs $Ag/AgNO_3$ in acetonitrile solution for 1 equiv of oxidation produced the mixed-valence compound, as proven by its ESR spectrum. Solutions of this species have been used in subsequent studies.

The reaction of the bridged dicobalt complexes with O_2 both is interesting in its own right and provides support for the internal bridging role of the 4,4′-bipyridine. One-electron oxidation of the complex produces the previously described Co^{II}/Co^{III} mixed-valence species whose dioxygen reactions are given in eq 10 and 11. As Figure 10 shows, the gradual addition of O_2 to a

$$2SCo^{III}\text{-}BB\text{-}Co^{II} + O_2 \rightleftharpoons SCo^{III}\text{-}BB\text{-}Co^{III}\text{-}O_2^{2-}\text{-}Co^{III}\text{-}BB\text{-}Co^{III}S \quad (10)$$

$$SCo^{III}\text{-}BB\text{-}Co^{III}\text{-}O_2^{2-}\text{-}Co^{III}\text{-}BB\text{-}Co^{III}S + O_2 \rightleftharpoons 2SCo^{III}\text{-}BB\text{-}Co\text{-}O_2 \quad (11)$$

solution of this complex in acetonitrile at −38 °C yields the expected spectral changes. The process is reversible under these conditions; however, close inspection of the spectral region around 480 nm reveals the presence of two distinct isosbestic points, 482 nm for P_{O_2} = 0–37.1 Torr and 485 for higher pressures (up to 742.3 Torr). The two changes are rationalized by eq 10 and 11, and the ESR spectral behavior of the system confirms this conclusion. The first set of ESR spectra in Figure 11 corresponds to the P_{O_2} range 0–19 Torr, and the spectra show that the cobalt(II) forms a diamagnetic, ESR-silent, 2:1 adduct at these low O_2 partial pressures. It is only when the partial pressure of O_2 is raised above 37 Torr that substantial amounts of the 1:1 Co/O_2 adduct are formed, as is demonstrated in the second set of ESR spectra in Figure 11.

(20) Sutton, J. E.; Taube, H. *Inorg. Chem.* **1981**, *20*, 3125–3134.

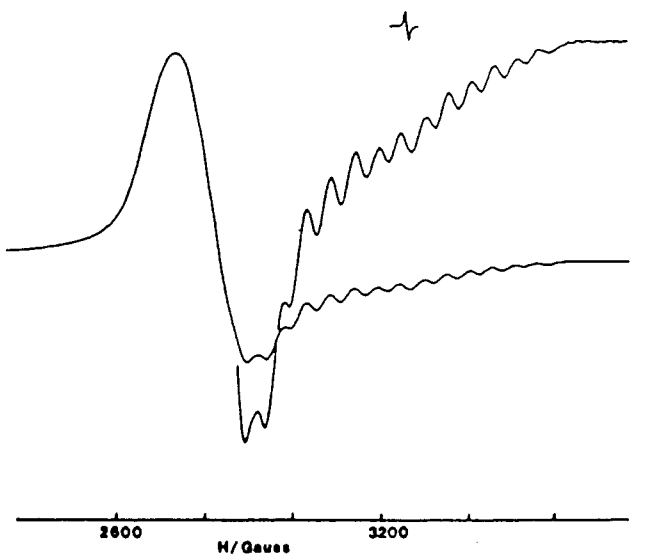

Figure 9. ESR spectrum of $[Co_2(4,4'\text{-bpy})\{(Me_2(NH)_2mxyl)_2([16]cyclidene)_2\}]^{4+}$ (in acetone containing $(n\text{-Bu})_4NBF_4$; ESR recorded at 77 K).

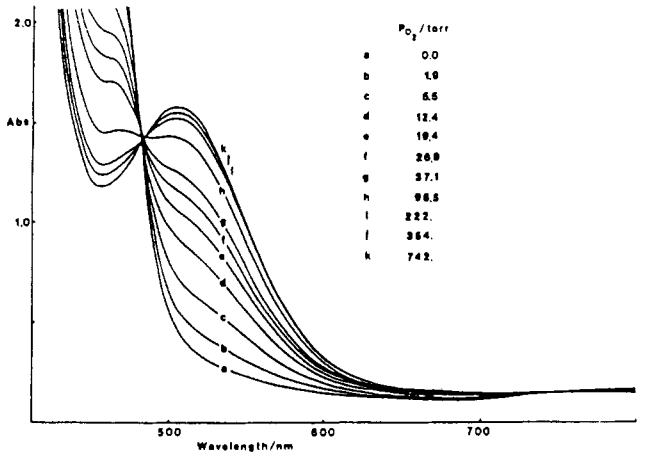

Figure 10. Visible absorption spectral changes of $[Co_2(4,4'\text{-bpy})\{(Me_2(NH)_2mxyl)_2([16]cyclidene)_2\}]^{5+}$ in acetonitrile upon exposure to various pressures of oxygen at −38 °C.

The behavior of the mixed-valence, guest-bridged complex as a fairly stable oxygen carrier is in marked contrast to that of the parent binuclear host–guest complex itself. That dicobalt(II) species rapidly suffers autoxidation of one of its two cobalt centers. The marked resistance toward autoxidation of the mixed-valence product can be rationalized in terms of the low electron density at cobalt(II) due to the electron withdrawal by the cobalt(III) center via the bridging base. That is, the effect is due to the presence of a very special axial base.

Experimental Section

Materials and Methods. Electronic spectra were recorded with either a Cary 17D or Varian 2300 spectrophotometer using a 1 cm gastight quartz cell, from Precision Cells, Inc. Hicksville, NY, fitted with a gas inlet. Oxygen partial pressures were achieved by the admixture of oxygen and nitrogen through a series of calibrated rotamers (Matheson, Inc.). Temperatures were maintained within ±0.2 °C by utilizing a Neslab or FTS constant-temperature circulation system with methanol as the coolant. A copper–constantan thermocouple was used to read temperature at the sample holder in the spectrophotometer chamber.

Electron spin resonance spectra were obtained on a Varian E-112 spectrometer operating at ~9.3 GHz. The spectra were calibrated with the DPPH radical, g = 2.0036. Oxygenations of the complexes were achieved in the same manner as that of the electronic spectroscopic experiments and were performed at the quoted temperatures prior to freezing in liquid nitrogen.

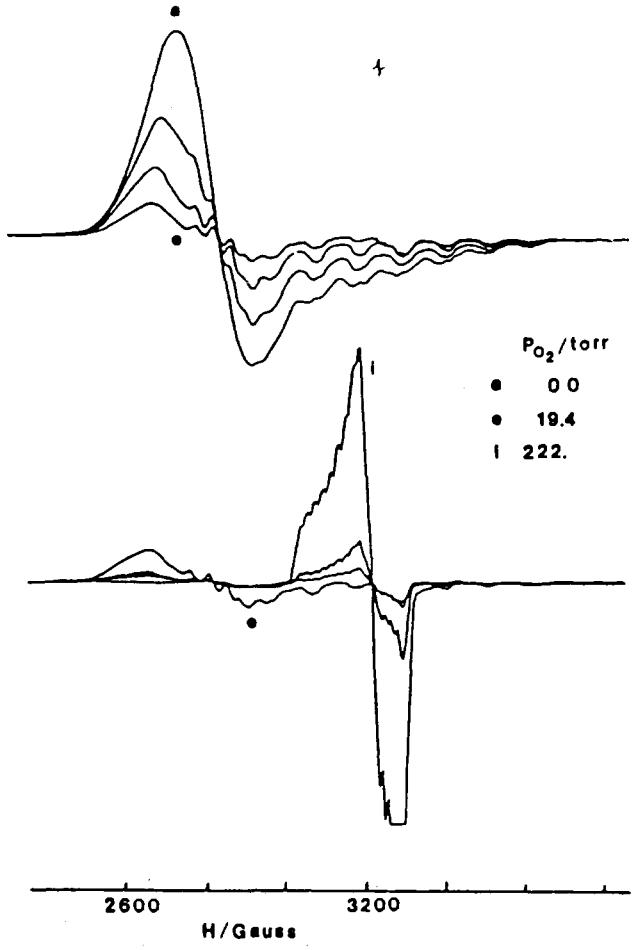

Figure 11. ESR spectral changes of $[Co_2(4,4'\text{-bpy})\{(Me_2(NH)_2mxyl)_2([16]cyclidene)_2\}]^{5+}$ in acetonitrile upon exposure to various pressures of oxygen at −40 °C.

All chemicals used in this work were of reagent grade or higher quality. All synthetic and preparatory manipulations were carried out in a Vacuum Atmospheres controlled-atmosphere chamber. The atmosphere was dry, oxygen-free nitrogen. Microanalyses were performed by Galbraith Laboratories, Knoxville, TN.

Synthesis of 2,7,9,15,17,22,24,30-Octamethyl-3,6,10,14,18,21,25,29,32,36,39,43-dodecaazatricyclo[21.7.7.7^{8,16}]tetratetraconta-1,7,9,14,16,22,24,29,31,36,38,43-dodecaeneoctayl Chloride Hexafluorophosphate, $[H_8\{(Me_2(NH)_2CH_2CH_2)_2([16]cyclidene)_2\}]Cl_x(PF_6)_{8-x}$. $[Ni_2\{(Me_2(NH)_2CH_2CH_2)_2([16]cyclidene)_2\}](PF_6)_4$ (2.0 g, 1.3 mmol) was dissolved in 200 mL of acetonitrile through which HCl gas was passed for 20 min. The color of the solution changed from amber to blue-green. The solvent was removed in vacuo, and the residual oil was taken up in 100 mL of water. To this resulting solution NH_4PF_6 (2.0 g, 12 mmol) was added with the temperature at 0 °C. A white precipitate formed immediately and was collected and washed, consecutively, with cold water, 2-propanol, and ether. The product was dried in vacuo. Yield: 1.2 g.

Synthesis of 2,12,14,20,22,32,34,40-Octamethyl-3,11,15,19,23,31,35,39,42,46,50,54-dodecaazapentacyclo-[31.7.7.7^{13,21}.1^{5,9}.1^{25,29}]hexapentaconta-1,5,7,9(48),12,14,19,21,25,27,29-(56),32,34,39,41,46,49,54-octadecaeneoctayl Bromide, $[H_8\{(Me_2(NH)_2mxyl)_2([16]cyclidene)_2\}]Br_8$. Through a methanolic slurry (20 mL) of $[Ni_2\{(Me_2(NH)_2mxyl)_2([16]cyclidene)_2\}](PF_6)_4$ (1.0 g, 0.64 mmol), hydrogen bromide gas was bubbled. The resulting white precipitate was collected, washed with methanol, and air-dried. The infrared spectrum of the product verified the absence of the PF_6 anion. Yield: 0.84 g, 87%.

Synthesis of (2,7,9,15,17,22,24,30-Octamethyl-3,6,10,14,18,21,25,29,32,36,39,43-dodecaazatricyclo[21.7.7.7^{8,16}]tetratetraconta-1,7,9,14,16,22,24,29,31,36,38,43-dodecaene-κ^8N)dicobalt(II) Chloride Tris(hexafluorophosphate), $[Co_2\{(Me_2(NH)_2CH_2CH_2)_2([16]cyclidene)_2\}]Cl(PF_6)_3$. The ligand salt $[H_8\{(Me_2(NH)_2CH_2CH_2)_2([16]cyclidene)_2\}]Cl_x(PF_6)_{8-x}$ (0.94 g) was slurried in 30 mL of warm methanol. To this slurry was added a mixture of 0.33 g (1.3 mmol) of $Co(CH_3CO_2)_2\cdot 4H_2O$ and 0.30 g (3.7 mmol) of $Na(CH_3CO_2)$ dissolved in 20 mL of methanol. The resulting orange-red solution was refluxed for 1 h, during which time an orange microcrystalline solid precipitated. Following cooling to room temperature, the product was collected and recrystallized from an acetonitrile/ethanol solution. Yield: 0.54 g, 71% based on a ligand salt with $x = 2$. Anal. Found (calcd) for: $C_{40}H_{64}N_{12}F_{18}P_3ClCo_2\cdot CH_3OH\cdot H_2O$: Co, 8.71 (8.72); C, 36.48 (36.44); H, 5.25 (5.22); N, 12.20 (12.44); Cl, 2.56 (2.62).

Synthesis of (2,3,6,7,9,15,17,18,21,22,24,30-Dodecamethyl-3,6,10,14,18,21,25,29,32,36,39,43-dodecaazatricyclo[21.7.7.7^{8,16}]tetratetraconta-1,7,9,14,16,22,24,29,31,36,38,43-dodecaene-κ^8N)dicobalt(II) Hexafluorophosphate, $[Co_2\{(Me_2(NMe)_2CH_2CH_2)_2([16]cyclidene)_2\}](PF_6)_4$. Under the same conditions as for the preceding reaction, $[H_8\{(Me_2(NMe)_2CH_2CH_2)_2([16]cyclidene)_2\}]Cl_x(PF_6)_{8-x}$ (0.63 g), $Co(CH_3CO_2)_2\cdot 4H_2O$ (0.22 g, 0.88 mmol), and $Na(CH_3CO_2)\cdot 3H_2O$ (0.36 g, 2.6 mmol) were used. The product, however, did not precipitate from the reaction mixture. A red residue resulted from the removal of solvent. This residue was extracted with acetonitrile (50 mL) and applied to a neutral alumina chromatography column. Following elution with acetonitrile and reduction of volume to 10 mL, ethanol was added to turbidity. An orange solid formed on standing. Yield: 0.23 g, 43% based upon a ligand salt with $x = 2$. Anal. Found (calcd) for $C_{44}H_{72}N_{12}F_{24}P_4Co_2$: Co, 7.83 (8.04); C, 35.83 (36.03); H, 4.98 (4.95); N, 11.56 (11.46).

Synthesis of (2,8,10,16,18,24,26,32-Octamethyl-3,7,11,15,19,23,27,31,34,38,41,45-dodecaazatricyclo[23.7.7.7^{9,17}]hexatetraconta-1,8,10,15,17,24,26,31,33,38,40,45-dodecaene-κ^8N)dicobalt(II) Hexafluorophosphate, $[Co_2\{(Me_2(NH)_2(CH_2)_3)_2([16]cyclidene)_2\}](PF_6)_4$. This complex was prepared in the same manner as the last-mentioned molecule by using 0.80 g of the homologous, mixed chloride/hexafluorophosphate ligand salt. Yield: 0.36 g. Anal. Found (calcd) for $C_{42}H_{68}N_{12}F_{24}P_4Co_2$: C, 33.74 (35.04); H, 4.76 (4.76); N, 11.70 (11.68); Co, 7.64 (8.19).

Synthesis of (2,12,14,20,22,32,34,40-Octamethyl-3,11,15,19,23,31,35,39,42,46,50,54-dodecaazapentacyclo-[31.7.7.7^{13,21}.1^{5,9}.1^{25,29}]hexapentaconta-1,5,7,9(48),12,14,19,21,25,27,29-(56),32,34,39,41,46,49,54-octadecaene-κ^8N)dicobalt(II) Hexafluorophosphate, $[Co_2\{(Me_2(NH)_2mxyl)_2([16]cyclidene)_2\}](PF_6)_4$. To a warm, methanolic slurry of $[H_8\{(Me_2(NH)_2mxyl)_2([16]cyclidene_2[]Br_8$ (0.77 g, 0.51 mmol) were added $Co(CH_3CO_2)_2\cdot 4H_2O$ (0.36 g, 1.4 mmol) and $Na(CH_3CO_2)\cdot 3H_2O$ (0.74 g, 5.4 mmol). The resulting deep red solution was then refluxed for 20 min at which time an orange precipitate formed. The solid was collected, washed with ethanol, and dried in vacuo.

To convert the above mixed anionic species, the solid was dissolved in 30 mL of 5/1 methanol/water and added to a saturated, methanolic solution of NH_4PF_6. The subsequently formed orange precipitate was then collected. Yield: 0.59 g (69%). Anal. Found (calcd) for $C_{52}H_{72}N_{12}F_{24}P_4Co_2\cdot 6H_2O$: C, 37.58 (37.38); H, 5.26 (5.07); N, 9.82 (10.06); Co, 7.05 (7.05).

Synthesis of (μ-4,4'-Bipyridine)(2,12,14,20,22,32,34,40-octamethyl-3,11,15,19,23,31,35,39,42,46,50,54-dodecaazapentacyclo-[31.7.7.7^{13,21}.1^{5,9}.1^{25,29}]hexapentaconta-1,5,7,9(48),12,14,19,21,25,27,29-(56),32,34,39,41,46,49,54-octadecaene-κ^8N)dicobalt(II) Dibromide Bis(hexafluorophosphate), $[Co_2(\mu\text{-}4,4'\text{-bpy})\{(Me_2(NH)_2mxyl)_2([16]cyclidene)_2\}]Br_2(PF_6)_2$. A 0.5-g sample of the bromide salt of the above *m*-xylylene-linked complex as a host was slurried in 20 mL of a 1:1 methanol–water mixture. To this was added 0.45 g (2.3 mmol) of 4,4'-bipyridine dihydrate. The resulting dark red solution was refluxed for 30 min, cooled, and stirred for an additional 60 min. The solution was then filtered. To the filtrate was slowly added NH_4PF_6 (1.0 g) in 8 mL of a 1:1 methanol–water mixture. A yellow powder was obtained. The product was isolated, washed extensively with methanol, and dried in vacuo. Yield: 0.59 g (90% based upon the ligand octahydrobromide). Anal. Found (calcd) for $C_{62}H_{80}N_{14}F_{12}P_2Co_2Br_2\cdot CH_3OH\cdot 6H_2O$: C, 43.70 (43.76); H, 5.61 (5.60); N, 11.22 (11.34); Co, 6.85 (6.82).

Crystal Structure Determination of $[Co_2\{(Me_2(NH)_2mxyl)_2([16]cyclidene)_2\}]Cl_4\cdot 2CH_3OH$. Red plates were grown by the evaporation of a methanolic solution. A suitable crystal (0.10 × 0.20 × 0.27 mm) was chosen for the experiment. The crystal was inserted in a 0.5-mm glass capillary that was then sealed with an epoxy cement. Crystal data are listed in Table V. Preliminary precession photographs indicated monoclinic symmetry with systematic absences attributable to the space group $P2_1/c$. Unit cell dimensions were determined by the accurate centering of 15 reflections well dispersed throughout reciprocal space. The data were collected by using a θ–2θ scan with scan rates varying between 2 and 12°/min, depending upon the intensity of a 2-s prescan. The scan range was 1.0° − Kα_1 to 1.0° + Kα_2, with background counts taken with a background-to-scan ratio of 0.5 at the beginning and end of each scan. Intensities and standard deviations were calculated according to the formula $I = r(S - RB)$ and $\sigma(I)^2 = r^2(S + R^2B)$, respectively, with r as the scan rate, S as the total scan count, R as the scan-to-background time ratio, and B as the total background count. Six standard reflections, monitored every 100 reflections, indicated no loss

Table V. Crystallographic Data for $[Co_2\{(Me_2(NH)_2mxyl)_2([16]cyclidene)_2\}]Cl_4 \cdot 2CH_3OH$

formula	$Co_2C_{52}H_{64}N_{12}Cl_4 \cdot 2CH_3OH$
fw	1180.95
cell params	
a, Å	11.121 (1)
b, Å	13.738 (3)
c, Å	20.185 (2)
α, deg	90
β, deg	99.15 (1)
γ, deg	90
V, Å^3	3044.6
Z	2
space group	$P2_1/c$
F_{000}	1202.0
D_{calcd}, g cm^{-3}	1.287
D_{obsd}, g cm^{-3}; method	1.30 (1); flotation in CCl_4/heptane
radiation	Mo Kα
2θ range, deg	$4 \le 2\theta \le 44$
no. of obsd reflcns ($I \ge 3\sigma(I)$)	1623
no. of params	164
final R factor	
R	0.070
R_w	0.080
goodness of fit (GOF)	4.426

of scattering power of the crystal. The data were corrected for background and Lorentz and polarization effects. Programs XRAY-70 and CRYM were used. The Wilson method was used to bring F^2 to a relatively absolute scale. The I^2 were scaled by increasing the I^2 obtained from counting statistics by PI^2, where P was chosen as the rms deviation of the standard reflections. Scattering factors were taken from the literature.[21,22]

The structure was solved by conventional heavy-atom methods. The positions of the remaining non-hydrogen atoms were revealed by subsequent Fourier syntheses. Refinement was performed by using full-matrix least-squares techniques during which the function $\sum(w(|F_o| - |F_c|))^2$ was minimized. The data were weighted according to $1/(\sigma_F)^2$. Residuals were calculated as $R = \sum||F_o| - |F_c||/\sum|F_o|$, and $R_w = (\sum w(|F_o| - |F_c|)^2/\sum w|F_o|^2)^{1/2}$. Isotropic refinement converged at $R = 0.073$. At this point, the thermal parameters of the cobalt and chlorine were allowed to vary anisotropically. The remaining atoms were constrained to be isotropic scatterers owing to the limited size of the data set. Subsequent full-matrix least-squares refinement converged to the herewith reported determination with $R = 0.070$ and $R_w = 0.080$. In the final cycle of refinement, no atom shifted more than 0.08 of any associated esd. A final difference Fourier map was featureless.

Acknowledgment. We wish to thank Dr. Thomas J. Meade for his assistance in magnetic susceptibility measurements. We are also grateful to Dr. J. Gallucci for the collection of X-ray diffraction data. The support of the National Institutes of Health is gratefully acknowledged.

Supplementary Material Available: A complete listing of observed and calculated structure factors (25 pages). Ordering information is given on any current masthead page.

(21) Stewart, R. F.; Davidson, E. R.; Simpson, W. T. *J. Chem. Phys.* **1965**, *42*, 3175-3187.
(22) (a) Cromer, D. T.; Mann, J. B. *Acta Crystallogr., Sect. A: Cryst. Phys., Diffr., Theor. Gen. Crystallogr.* **1968**, *A24*, 321-324. (b) *International Tables for X-Ray Crystallography*; Ibers, J. A., Hamilton, W. C., Eds.; Kynoch: Birmingham, England, 1974; Vol. 1, pp 149-150.

Contribution from the Departments of Chemistry, The University of North Carolina, Chapel Hill, North Carolina 27514, and The University of Wyoming, Laramie, Wyoming 82071

Barium Binding to γ-Carboxyglutamate and β-Carboxyaspartate Residues: Structures of Barium Complexes of Benzylmalonate, Dimethylmalonate, and Ethylmalonate Ions

Yoshinobu Yokomori,[1a,b] Kathleen A. Flaherty,[1a] and Derek J. Hodgson*[,1c]

Received October 14, 1987

The molecular structures of four barium complexes of substituted malonate ions have been determined from X-ray diffraction data. The 1:2 benzylmalonate complex $Ba(bzmalH)_2 \cdot H_2O$, $Ba(C_{10}O_4H_9)_2 \cdot H_2O$, crystallizes in the orthorhombic space group $Cmc2_1$ with four molecules in a cell of dimensions $a = 34.085$ (13) Å, $b = 7.153$ (2) Å, and $c = 9.024$ (5) Å, and its structure has been refined to a final R factor of 0.050. The 1:1 complex $Ba(bzmal) \cdot 3H_2O$, $BaC_{10}O_4H_8 \cdot 3H_2O$, crystallizes in the monoclinic space group $P2_1/c$ with four molecules in a cell of dimensions $a = 14.373$ (3) Å, $b = 5.489$ (4) Å, $c = 16.892$ (3) Å, and $\beta = 111.4$ (1)°, and its structure has been refined to an R factor of 0.074. The 1:1 dimethylmalonate complex $[Ba(dmal)]_2 \cdot 5H_2O$, $Ba_2(C_5O_4H_6)_2 \cdot 5H_2O$, crystallizes in the monoclinic space group $P2_1/n$ with four molecules in a cell of dimensions $a = 6.194$ (7) Å, $b = 22.010$ (16) Å, $c = 13.225$ (7) Å, and $\beta = 95.62$ (5)°, and its structure has been refined to an R factor of 0.060. The 1:2 ethylmalonate complex $Ba(emalH)_2 \cdot H_2O$, $BaC_{10}O_8H_{14} \cdot H_2O$, is orthorhombic, of space group *Pnma*, with four molecules in a cell of dimensions $a = 10.829$ (2) Å, $b = 26.542$ (10) Å, and $c = 4.760$ (8) Å and has been refined to an R factor of 0.034. All four complexes are polymeric, revealing all three of the possible modes of binding of a metal ion to a dicarboxylate moiety. The significance of these structural features in determining the binding strengths of normal and abnormal prothrombin in barium salts is discussed, as is the distinction between the binding of magnesium and beryllium on the one hand and calcium and barium on the other.

The existence and biological significance of both γ-carboxyglutamic (Gla) and β-carboxyaspartic (Asa) acid residues in numerous proteins are well documented,[2-8] although the precise reason(s) for these posttranslational carboxylations is not completely understood. It is, however, well established that Gla residues are implicated in calcium binding,[9] although an equally important function may be to provide sites for interactions with neighboring arginine (Arg) residues, thereby bringing about conformational changes necessary for protein function.[10] It is also known that calcium ions, while binding to the Gla residues,

(1) (a) The University of North Carolina. (b) Permanent address: Department of Chemistry, The National Defense Academy, Hashirimizu, Yokosuka 239, Japan. (c) The University of Wyoming.
(2) Magnusson, S.; Sottrup-Jensen, L.; Peterson, T. E.; Morris, H. R.; Dell, A. *FEBS Lett.* **1974**, *44*, 189-193.
(3) Stenflo, J.; Fernlund, P.; Egan, W.; Roepstorff, P. *Proc. Natl. Acad. Sci. U.S.A.* **1974**, *71*, 2730-2733.
(4) Prendergast, F. G.; Mann, K. G. *J. Biol. Chem.* **1977**, *252*, 840-850.
(5) Suttie, J. W.; Jackson, C. M. *Physiol. Rev.* **1977**, *57*, 1-70.
(6) Lian, J. B.; Hauschka, P. V.; Gallop, P. M. *Fed. Proc., Fed. Am. Soc. Exp. Biol.* **1978**, *37*, 2615-2620.
(7) Christy, M. R.; Barkley, R. M.; Koch, T. H.; Van Buskirk, J. J.; Kirsch, W. M. *J. Am. Chem. Soc.* **1981**, *103*, 3935-3937.
(8) Christy, M. R.; Koch, T. H. *J. Am. Chem. Soc.* **1982**, *104*, 1771-1772.
(9) Jackson, C. M.; Nemerson, Y. *Annu. Rev. Biochem.* **1980**, *49*, 765-811.
(10) Craig, D. H.; Koehler, K. A.; Hiskey, R. G. *J. Org. Chem.* **1983**, *48*, 3954-3960.

0020-1669/88/1327-2300$01.50/0